Inorganic Chemistry

Article

pubs.acs.org/IC

Bottleneck Effect of *N,N*-Dimethylformamide in InOF-1: Increasing CO_2 Capture in Porous Coordination Polymers

Elí Sánchez-González,[†] Eduardo González-Zamora,[*,§] Diego Martínez-Otero,[‖] Vojtech Jancik,[*,‖] and Ilich A. Ibarra[*,†]

[†]Laboratorio de Fisicoquímica y Reactividad de Superficies (LaFReS), Instituto de Investigaciones en Materiales, Universidad Nacional Autónoma de México, Circuito Exterior s/n, CU, Del Coyoacán, 04510, México D.F., México

[§]Departamento de Química, Universidad Autónoma Metropolitana—Iztapalapa, San Rafael Atlixco 186, Col. Vicentina, Iztapalapa, C.P., 09340 Ciudad de México, Mexico

[‖]Centro Conjunto de Investigación en Química Sustentable UAEM−UNAM, Personal del Instituto de Química de la UNAM, Carr. Toluca-Atlacomulco Km 14.5, Toluca, Estado de México 50200, México

Supporting Information

ABSTRACT: The bottleneck effect of confined *N,N*-dimethylformamide (DMF) molecules was observed in InOF-1 for the first time: CO_2 capture was remarkably enhanced in samples of as-synthesized InOF-1, thermally activated in such a way that a small residual amount of DMF molecules remained confined within the pores (DMF@InOF-1). Dynamic CO_2 adsorption experiments on DMF@InOF-1 exhibited a CO_2 capture of 8.06 wt % [1.5-fold higher than that of a fully activated InOF-1 (5.24%)]. DMF@InOF-1 can reversibly adsorb/desorb 8.09% CO_2 with no loss of CO_2 capacity after 10 cycles, and the desorption is accomplished by only turning the CO_2 flow off. Static CO_2 adsorption experiments (at 196 K) demonstrated a 1.4-fold CO_2 capture increase (from 5.5 mmol·g^{-1}, fully activated InOF-1, to 7.5 mmol·g^{-1}, DMF@InOF-1). Therefore, these CO_2 capture properties are the result of the presence of residual-confined DMF molecules within the InOF-1 framework and their interactions via a very strong hydrogen bond with the $In_2(\mu$-OH) groups, which prevent DMF leaching. The stability of this hydrogen bond is given by a perfect fit of the DMF molecule in the "dent" around the OH group that allows a nearly ideal orientation of the DMF molecule towards the OH group.

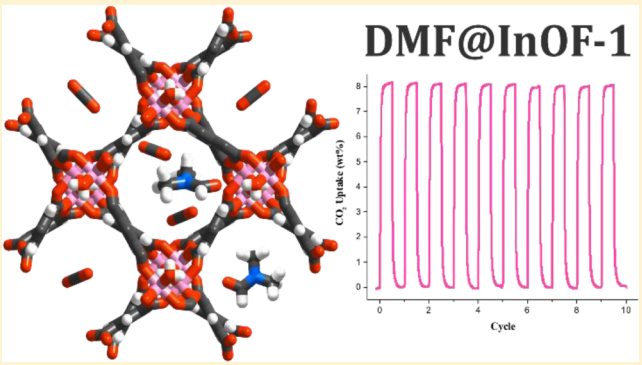

INTRODUCTION

The growth in atmospheric CO_2 over the past decades is a result of increasing and indiscriminate fossil-fuel combustion.[1] In 2015, global CO_2 emissions have augmented up to 35.7 billion tonnes per year, and 90% of these emissions are solely associated with fossil-fuel combustion.[2] The continuous rise in CO_2 emissions is directly connected to the continuous rise of temperature across the planet, which contributes to one of the highest threats to our civilization: global warming. Unfortunately, the CO_2 concentration in the atmosphere is expected to increase before a noncarbon-containing fuel takes over as the dominant energy resource.[2] Given our high degree of dependence on fossil fuels and the technical, economic, and social difficulties of large-scale use of alternative energy options, a drastic reduction of atmospheric CO_2 emissions is essential to minimize the related risks that global warming represents to our planet.

The direct capture of CO_2 from a very concentrated CO_2 stationary source is technically possible and could be potentially cost-effective. For example, in a typical power plant, the composition of flue gas is CO_2 (10−15%), NO (1500−2500 ppm), and SO_2 (500−2000 ppm).[3] NO is transformed by selective catalytic reduction, SO_2 is captured by a wet lime scrubber, and CO_2 is vented to the atmosphere.[4] Therefore, international leaders are intensively boosting many environmental initiatives for the development of new CO_2 capture technologies.[5] Current technological strategies for CO_2 capture are mainly based on CO_2 absorption in aqueous amines with many disadvantages such as the corrosion of pipelines, heat instability, and high cost for their regeneration.[6] The cost of CO_2 sequestration can be considerably reduced if an effective CO_2 capture sorbent system is established with the following characteristics: (i) high CO_2 capture capacity (>1000 μmol·g^{-1}) and (ii) long-term regeneration capacity.[7] Poliakoff et al.[8] postulated "the 12 principles of CO_2 chemistry", where CO_2 capture corresponds to one of these principles (*maximize*

Received: February 28, 2017
Published: April 27, 2017

DOI: 10.1021/acs.inorgchem.7b00519
Inorg. Chem. 2017, 56, 5863−5872

integration) and the use of porous solid materials for this task represents a very promising alternative.

Porous coordination polymers (PCPs) or metal−organic frameworks (MOFs) are highly crystalline materials that show high structure stability, adsorption capacity, and mild regeneration conditions for CO_2 capture and separation.[9] Enhancement of CO_2 capture in PCPs can be achieved by optimizing intrapore interactions between these materials and CO_2 molecules.[10] Typical synthetic strategies to improve host−guest interactions in PCP materials are based on the functionalization of pores with basic (Lewis) nitrogen-containing groups such as triazole,[11] amine,[10a,12] and tetrazole[13] and the generation of acid (Lewis) open metal sites.[14]

The confinement of solvents inside porous solid supports represents a new and exciting synthetic strategy to improve CO_2 capture.[15] Because the physical properties of the solvents strongly depend on the system scale, the confinement of these in nanostructures considerably modifies their viscosity, density, dielectric constant, and specific heat.[16] For example, Luzar and Bratko[17] predicted [by performing molecular dynamics (MD) computer simulations] a 15-fold increase in CO_2 capture via the confinement of H_2O in a hydrophobic environment. Pellenq et al.[15] confined *N*-methyl-2-pyrrolidone in a mesoporous material, entitled MCM-41, and demonstrated a 6-fold increase in the CO_2 solubility. Remarkably, Llewellyn et al.[18] reported a 5-fold increase in CO_2 capture by the confinement of H_2O in MIL-100(Fe). Similarly, Walton et al.[19] demonstrated that controlled H_2O adsorption can enhance CO_2 capture in PCPs by incorporating functional groups within the pores of these materials. They showed that hydroxyl (−OH) functional groups act as directing agents for H_2O molecules inside the pores, allowing a more efficient and ordered packing of H_2O.[20] Furthermore, Yaghi et al.[21] proposed that the presence of these functional groups (−OH) improves the affinity of PCP materials to H_2O.

We are interested in developing hybrid adsorbent PCP materials capable of sequestering large amounts of CO_2 (via confinement of DMF in the pores of PCPs) in parallel with our previous studies, where H_2O[22] and ethanol (EtOH)[23] were confined within the micropores of PCPs, to increase CO_2 capture. In fact, when solvent molecules are confined within PCPs, they partially block their micropores, and this phenomenon results in an enhanced CO_2 capture (due to a more efficient CO_2 packing within PCPs); we designated this singularity as the "bottleneck effect".[23] Conversely to the standard procedure of solvent exchange after PCP materials have been synthesized, herein we report the direct use of thermally activated samples of InOF-1,[24] which contain a small residual amount of DMF within the pores of the PCP material. InOF-1 crystallizes in the chiral space group $I4_122$, and it is based on a binuclear [$In_2(\mu_2$-OH)] building block.[24] Each indium(III) center adopts an octahedral coordination environment, with four oxygen donors from four different $BPTC^{4-}$ ligands (H_4BPTC = biphenyl-3,3′,5,5′-tetracarboxylic acid)[25] and two μ_2-OH groups. InOF-1 shows a 3D framework structure with channel openings of approximately 7.5 Å (considering the van der Waals radii of the surface atoms). In this contribution, we report for the first time, to the best of our knowledge, the CO_2 capture enhancement properties of InOF-1 by confining DMF within its micropores, along with the precise localization of DMF molecules, via single-crystal X-ray diffraction experiments.

EXPERIMENTAL SECTION

Chemicals. Indium nitrate [$In(NO_3)_3$], biphenyl-3,3′,5,5′-tetracarboxylic acid (H_4BPTC), *N*,*N*-dimethylformamide (DMF), acetonitrile (CH_3CN), and nitric acid (HNO_3, 65%) were purchased from Sigma-Aldrich and used as received.

Material Synthesis. $In_2(OH)_2$(BPTC) (InOF-1, where BPTC = biphenyl-3,3′,5,5′-tetracarboxylate) was synthesized according to previously reported procedures:[24] $In(NO_3)_3$ (156 mg, 0.40 mmol) and H_4BPTC (33 mg, 0.10 mmol) were dissolved in CH_3CN (5 mL), DMF (5 mL), and HNO_3 (65%, 0.2 mL) and sealed in a pressure tube. The clear solution was heated at 358 K in an oil bath for 72 h. The tube was cooled to room temperature over a period of 12 h, and the colorless crystalline product was separated by filtration, washed with DMF (5 mL), and dried in air. Yield: 72% (based on the ligand). Thermogravimetric analysis (TGA) and powder X-ray diffraction (PXRD) were carried out to assess the purity of the material (see Figures S1 and S2 in the Supporting Information).

Adsorption Isotherms for N_2, CO_2, and H_2O. N_2 isotherms (up to 1 bar and 77 K) were recorded on a Belsorp mini II analyzer under high vacuum in a clean system with a diaphragm pumping system. CO_2 isotherms up to 1 bar and 196 K were recorded on a Belsorp HP (high-pressure) analyzer. Ultrapure grade (99.9995%) N_2 and CO_2 gases were purchased from Praxair. H_2O isotherms were obtained with a humidity-controlled thermobalance (Q5000 SA, from TA) at 303 K.

Kinetic CO_2 Uptake Experiments. Kinetic experiments were performed by using a thermobalance (Q500 HR, from TA) at 303 K with a constant CO_2 flow (60 mL·min^{-1}).

Adsorption Microcalorimetry for CO_2. CO_2 adsorption microcalorimetry experiments were carried out on InOF-1, EtOH@InOF-1, and DMF@InOF-1 at 303 K. The evolved heat was measured using a Tian-Calvet microcalorimeter (CA-100, ITI). This instrument measures the CO_2 isotherm and the enthalpy of adsorption for CO_2 simultaneously using a point-by-point introduction of CO_2 gas to the sample.

Single-Crystal X-ray Diffraction Experiments. Single crystals of as-synthesized InOF-1 were obtained by slow cooling of the reaction mixture after its synthesis. These crystals were separated from the mother liquor, submerged in Paratone oil to protect them from moisture, and used for data collection. A selected crystal was mounted on a Bruker APEX DUO diffractometer equipped with an Apex II CCD detector at 100 K. Frames were collected using ω scans[26] and integrated with *SAINT*.[26] Multiscan absorption correction (*SADABS*)[26] was applied. The structures were solved by intrinsic phasing (*SHELXT*)[27] and refined using full-matrix least squares on F^2 with *SHELXL*[28] within the *ShelXle GUI*.[29] Weighted *R* factors, R_w, and all goodness-of-fit indicators are based on F^2. All non-hydrogen atoms were refined anisotropically. The hydrogen atoms of the C−H bonds were placed in idealized positions, whereas the hydrogen atom from the OH moiety was localized from the difference electron density map, and its position was refined with U_{iso} tied to the parent atom with distance restraint (DFIX). The disordered DMF molecule was refined using geometry (DFIX and SAME) and U_{ij} restraints (SIMU and RIGU) implemented in *SHELXL*.[28] The molecular graphics were prepared using *Mercury* and *GIMP*.[30] The surface of the "dent" was calculated with a probe radius of 1.5 Å and a grid spacing of 0.1 Å within *Mercury*.[31] CCDC 1518398 contains the supplementary crystallographic data for this paper. Copies of the data can be obtained free of charge via http:/www.ccdc.cam.ac.uk/const/retrieving.html or from the Cambridge Crystallographic Data Centre, 12 Union Road, Cambridge CB2 1EZ, U.K. [fax (+44)1223-336-033; e-mail deposit@ccdc.cam.ac.uk].

RESULTS AND DISCUSSION

Single-Crystal X-ray Diffraction Studies. In our previous study, we determined that the increment of CO_2 capture in InOF-1 is the result of a bottleneck effect due to the pores being partially filled by EtOH molecules hydrogen-bonded to the $In_2(\mu$-OH) group.[23] Thus, the crystal structure of the as-

DOI: 10.1021/acs.inorgchem.7b00519
Inorg. Chem. 2017, 56, 5863−5872

synthesized sample of InOF-1 was determined to unambiguously confirm the nature of the interaction of the InOF-1 framework with the DMF molecules (Table 1 and Figure 1).

Table 1. Selected Crystallographic Data for the As-Synthesized InOF-1

chemical formula	$C_{11}H_{11}InNO_6$
formula mass	368.03
cryst syst	tetragonal
a (Å)	15.4702(8)
b (Å)	15.4702(8)
c (Å)	12.3125(6)
α (deg)	90
β (deg)	90
γ (deg)	90
unit cell volume (Å^3)	2946.7(3)
temperature (K)	100(2)
space group	$I4_122$
wavelength (Å)	0.71073
Z	8
density (g·cm^{-3})	1.659
absorption factor (mm^{-1})	1.623
F(000)	1448
cryst size (mm^3)	0.246 × 0.106 × 0.060
θ range (deg)	2.114−28.281
limiting indices	$-20 \le h \le 20$, $-20 \le k \le 20$, $-16 \le l \le 16$
reflns collected	17397
reflns unique (R_{int})	1842 (0.0272)
no. of data/restraints/param	1842/62/121
GOF on F^2	1.125
R_1,[a] wR_2[b] [$I > 2\sigma(I)$]	0.0180, 0.0493
R_1,[a] wR_2[b] (all data)	0.0185, 0.0496
absolute structure param	0.21(5)
residual electron density (e·Å^{-3})	0.628/−0.316
SQUEEZE volume of the voids (Å^3)	568
SQUEEZE no. of removed electrons (e)	198

[a] $R_1 = \sum||F_o| - |F_c||/\sum|F_o|$. [b] $wR_2 = [\sum w(F_o^2 - F_c^2)^2/\sum(F_o^2)^2]^{1/2}$.

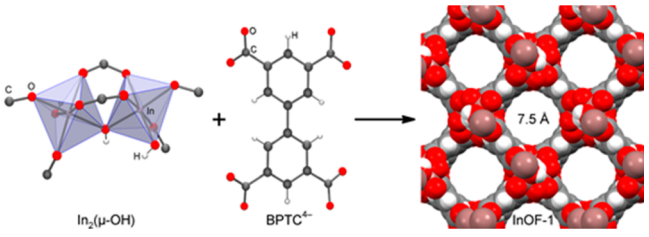

Figure 1. Views of the binuclear building block of two metal-ion oxygen octahedra bridged by a μ_2-hydroxo group (left), the $BPTC^{4-}$ ligand (center), and the crystal structure of InOF-1 along the c axis showing 7.5 Å channels (right).

As expected, the $In_2(\mu$-OH) group forms a hydrogen bond with the DMF molecule; however, in contrast to the hydrogen-bonded EtOH molecule in our previous study,[23] the DMF molecule shows less disorder and is, in fact, involved only in a symmetry-induced disorder caused by its presence in the vicinity of a 2-fold axis. This substantial difference can be rationalized in terms of the present hydrogen bonding, the free space around the $In_2(\mu$-OH) group, and the shape of the solvent molecule. As can be seen in Figure 2, the −OH group is

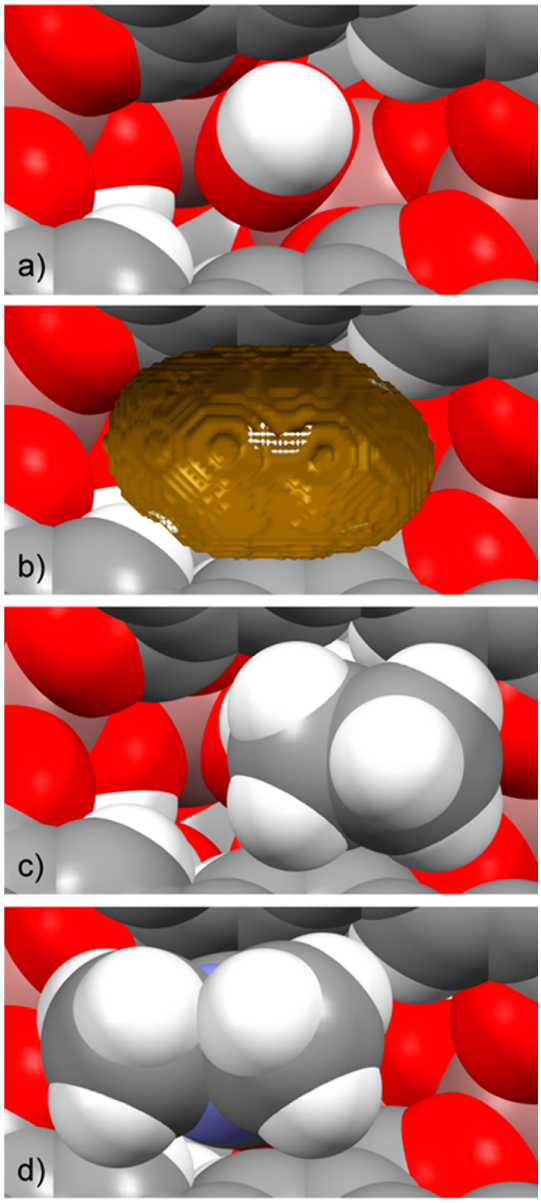

Figure 2. Space-filling model of (a) the close ambient of the $In_2(\mu$-OH) group (b) with 3D topology of the "dent", (c) with a hydrogen-bonded EtOH molecule, and (d) with a hydrogen-bonded DMF molecule.

located inside a "dent in the wall" created by two organic BPTC ligands bridging the same $In_4(\mu\text{-OH})_3$ unit. The shape of the dent is the main reason why DMF binds far more strongly to the −OH group than EtOH. The hydrogen bond is usually described by the O−H, O···O, and H···O distances and the O−H···O angle. These parameters are 0.83(1), 1.84(2), and 2.663(9) Å and 172(2)° for DMF and 0.84(1), 1.97(2), and 2.73(1) Å and 151(2)° for the main position of the EtOH molecule.[23]

In the case of EtOH, the geometry around its oxygen atom and specifically the presence of its acidic proton is not compatible with the form of the dent around the $In_2(\mu$-OH) group, and thus the EtOH molecule cannot assume an ideal position for hydrogen-bonding formation. That is visualized by a longer O···O distance and mainly by the C−O···H angle of 153° between the proton of the $In_2(\mu$-OH) group and the C−

DOI: 10.1021/acs.inorgchem.7b00519
Inorg. Chem. 2017, 56, 5863−5872

O fragment of the EtOH molecule. In the case of the perfect orientation of the EtOH molecule, this angle should be close to 109°.[23] On the other hand, the orientation of the DMF molecule is nearly perfect because the corresponding angle is with 115°, very close to the theoretical 120° value for sp^2 hybridization. Also, the O−H···O angle is nearly linear [172(2)°]. Additionally, the methyl group of the EtOH molecule is forced against the "dent's" wall (Figure 2c). All of this allows the DMF molecule to interact very strongly with the $In_2(\mu$-OH) group (Figure 3), explaining the high temperatures

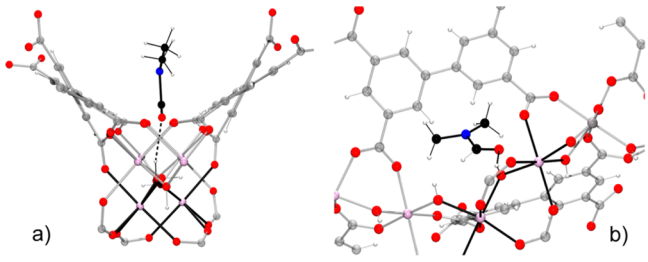

Figure 3. Mutual orientations of the DMF molecule and InOF-1 framework, showing the hydrogen bond between the DMF and $In_2(\mu$-OH) groups (a) in the direction of the channel and (b) showing details of the hydrogen bond.

(453 K) necessary for activation of the as-synthesized InOF-1 and the high stability of the DMF@InOF-1 [$In_2(OH)_2$(BPTC)·$DMF_{0.34}$] material during the repeated cycles of CO_2 adsorption/desorption. It is also worth noting that 4.2 wt % residual DMF in DMF@InOF-1 (vide supra) is equivalent to 1.37 DMF molecules per unit cell (0.17 DMF molecules per μ-OH group) and is practically identical with that found for the maximum bottleneck effect of EtOH in InOF-1 (1.35 EtOH molecules). Thus, in DMF@InOF-1, the adsorption of CO_2 is enhanced by the bottleneck effect, but simultaneously, the flow of CO_2 is not capable of breaking the hydrogen bond between the DMF molecule and the framework, suppressing DMF leaching and making this system reusable.

CO_2 Capture Studies. Dynamic and isothermal CO_2 experiments (kinetic) were carried out on InOF-1 (see Activation Methods in the Supporting Information). Figure 4 (InOF-1) shows the kinetic CO_2 uptake experiment at 303 K. At this temperature, the material showed the maximum weight percentage gain, which indicates the maximum amount of CO_2

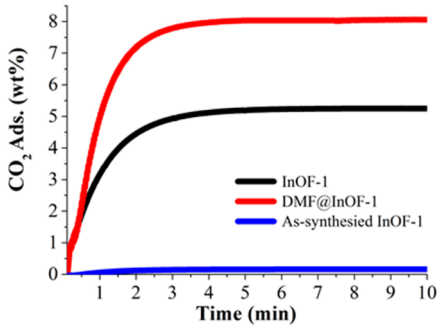

Figure 4. Kinetic CO_2 uptake experiments performed at 303 K with a CO_2 flow of 60 mL·min^{-1} in InOF-1 (black curve), DMF@InOF-1 (4.2 wt % DMF within the pores; red curve), and as-synthesized InOF-1 (blue curve).

captured. This amount corresponded to 5.24 wt %, and it was rapidly reached after only 5 min, remaining constant until the end of the experiment (10 min; Figure 4, InOF-1).

Later, a freshly synthesized sample of InOF-1 was activated (453 K for 1 h and under a flow of N_2) and cooled to 303 K (under N_2). Hereinafter, this sample will be referred to as DMF@InOF-1. It was decided to activate the as-synthesized InOF-1 samples at 453 K for 1 h with the goal of partially removing the DMF molecules from the pores of InOF-1. In fact, by running a high-definition TGA on an as-synthesized sample of InOF-1 [high-resolution (Hi-Res) mode with a heating rate of 5 K·min^{-1}, a Hi-Res setting of 5, and a sensitivity of 1], we managed to estimate the amount of residual DMF within the micropores of DMF@InOF-1 as 4.2 wt % [see Figure S3 (left) in the Supporting Information]. In order to confirm the reproducibility on the amount of residual DMF, five freshly synthesized samples of InOF-1 were analyzed with Hi-Res TGA, and the results are shown in Table S1 (see the Supporting Information). By taking the average of those five experiments, the residual DMF in InOF-1 corresponded to 4.242 wt % (see Table S1 in the Supporting Information). In fact, a fully activated sample of InOF-1 (4 days in acetone followed by 453 K and 10^{-3} bar for 1 h) was saturated with anhydrous DMF, and a TGA experiment [see Figure S3 (right) in the Supporting Information] showed that it can adsorb 28.2 wt % DMF.

Additionally, another fully activated sample of InOF-1 was saturated with anhydrous DMF, and Hi-Res TGA demonstrated that when this DMF-saturated sample reached 453 K, the residual amount of DMF within the pores of DMF corresponded to 6.7 wt % [see Figure S3 (left) in the Supporting Information]. This result showed that when the sample is fully activated, it can adsorb more DMF than the as-synthesized sample, and thus we decided to only work with as-synthesized samples of InOF-1. From the energy-savings and practical points of view, the direct use of as-synthesized samples of InOF-1 (with only a simple activation step) is much more attractive for any CO_2 capture studies than the much longer (at least 4 days) and energy-consuming solvent-exchange (e.g., acetone) process.

We previously reported that small amounts of H_2O[22] and EtOH,[23] within the micropores of PCPs, enhanced CO_2 capture. Therefore, we hypothesized that small amounts of DMF occluded inside the microporous channels of InOF-1 (DMF is "pinned" to the μ_2-OH functional groups via hydrogen bonding) could also improve the CO_2 adsorption capacity of the material. This hypothesis was also complemented by Paesani and co-workers,[32] who showed by computational IR spectroscopy that when the material MIL-53(Cr) is loaded with small amounts of H_2O, these can directly interact with the hydroxo (μ_2-OH) functional groups of the PCP material (hydrogen bonding).

By taking the approach of MD, Haigis et al.[33] proposed that H_2O molecules can form strong hydrogen bonds with the μ_2-OH functional groups, in MIL-53(Cr), as a function of H_2O loading. Additionally, Maurin et al.[34] corroborated by grand canonical Monte Carlo computational simulations, in MIL-53(Cr), that at low H_2O loadings these H_2O molecules are regularly accommodated inside all of the pores of the material.

Then, a kinetic CO_2 experiment (303 K) was carried out on DMF@InOF-1. The adsorption isotherm showed a two-step uptake for the DMF@InOF-1 sample (Figure 4). The first step (from 0 to approximately 0.5 min) showed a very fast CO_2

DOI: 10.1021/acs.inorgchem.7b00519
Inorg. Chem. 2017, 56, 5863−5872

uptake (~2 wt %), which indicates a high CO_2 affinity of the DMF@InOF-1 material. This affinity was experimentally corroborated by the molar enthalpy of adsorption (ΔH) for CO_2 (vide infra). The maximum amount of CO_2 captured was equal to 8.06 wt % and was achieved within approximately 5 min, and it was constant until the end of the experiment (Figure 4, DMF@InOF-1). Therefore, when there is a residual small amount of DMF (4.2 wt %), CO_2 capture (in InOF-1) was roughly 1.5-fold-augmented (from 5.24 to 8.03 wt %) in comparison to the fully activated InOF-1 sample. Furthermore, the CO_2 adsorption kinetics were considerably improved by the presence of the remaining DMF molecules, within the micropores of InOF-1, because the 1.5-fold increase was reached at the same time (approximately 5 min). Later, a freshly synthesized InOF-1 sample (without any activation protocol) was used for a kinetic CO_2 experiment at 303 K. The total amount of CO_2 captured was approximately equal to 0.1 wt % (Figure 4, as-synthesized InOF-1). In this case, the pores in the as-synthesized InOF-1 sample are filled with the reaction solvent mixture ($DMF/CH_3CN/H_2O$), and thus the inclusion of CO_2 molecules, into the micropores of the material, was not possible.

As it was stated before, for any CO_2 capture material, it is essential to show a long-term regeneration capacity with low-energy requirements for CO_2 release.[7] Certainly, this step is another fundamental factor in the cost of potential industrial separation processes.[35] In fact, different regeneration methodologies can be used depending on the characteristics of a given material. One of the most common methods is vacuum- and temperature-swing desorption. Long and co-workers[36] reported a working CO_2 capacity (total CO_2 adsorption) of approximately 7 wt % at 25 °C on mmen-CuBTTri. The PCP material was regenerated by switching the flow (15% CO_2 in N_2) to a pure N_2 stream followed by raising the temperature to 60 °C. This treatment was necessary because the enthalpy of adsorption for CO_2, for mmen-CuBTTri, was calculated to be ΔH = 96 kJ·mol^{-1} (very close to that of chemisorption formation, ca. 100 kJ·mol^{-1}), which indicates a very strong physisorption between CO_2 molecules and the pore walls of the material; therefore, more energy was required for CO_2 release. Yaghi et al.[37] reported on Mg-MOF-74 a working CO_2 capacity of 8.9 wt % with full regeneration of the material under purge-flow conditions at 80 °C. Denayer and co-workers[38] reported a separation capacity (total CO_2 adsorption) of 3.7 wt % for NH_2-MIL-53 with regeneration of the material at 159 °C under a purge flow.

To test the regeneration properties of DMF@InOF-1, a freshly synthesized sample was subjected to kinetic CO_2 adsorption/desorption experiments at 303 K (Figure 5). Each cycle consists of an adsorption step (15 min) and a desorption step (15 min), enabling a cycling time of only 30 min without the use of N_2 or high temperature.

When only the CO_2 flow was turned off (reducing the pressure: desorption step) at the same adsorption temperature (303 K), complete regeneration of the DMF@InOF-1 material was achieved with no loss of CO_2 capacity even after 10 adsorption/desorption cycles (average CO_2 adsorption = 8.09 wt %; Figure 5). This is a remarkable result because there is no need to use a purge gas (e.g., N_2) and, more importantly, no thermal reactivation of the sample is required, resulting in a very low-cost separation process. The isosteric enthalpy of adsorption for CO_2 on DMF@InOF-1 (molar enthalpy of adsorption, ΔH) was experimentally measured by CO_2

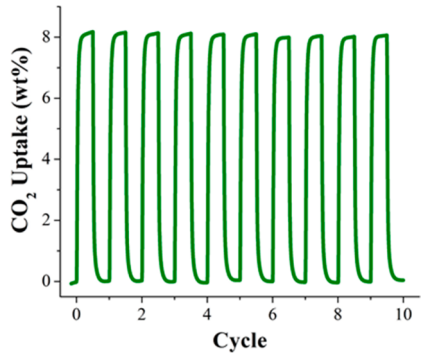

Figure 5. Adsorption/desorption cycling for DMF@InOF-1, demonstrating a reversible CO_2 uptake of 8.09 wt %.

adsorption microcalorimetry (see Figure S4 in the Supporting Information), giving a value of ΔH = 45.6 kJ·mol^{-1}, which is a characteristic value for a mild physisorption in PCPs.[5] In order to establish a comparison of the CO_2 affinity of this material (DMF@InOF-1) with InOF-1 and EtOH-impregnated InOF-1,[23] the isosteric enthalpy of adsorption for CO_2 for these two materials (InOF-1 and EtOH@InOF-1) was determined in the same way (see Figures S5 and S6 in the Supporting Information). The ΔH values for InOF-1 and EtOH@InOF-1 were 32.4 and 48.7 kJ·mol^{-1}, respectively. Thus, the DMF@InOF-1 material showed a value of the molar enthalpy of adsorption for CO_2 between the fully activated material (InOF-1) and the material impregnated with EtOH (EtOH@InOF-1) which is also in good agreement with the total CO_2 capture: InOF-1 (5.24 wt %) and EtOH@InOF-1 (14.14 wt %).[23] In addition, the Brunauer–Emmett–Teller (BET) surface area of EtOH@InOF-1 was calculated to be 514 m^2·g^{-1} with a pore volume of 0.28 cm^3·g^{-1} (see Table 2).

The heat of adsorption (ΔH) for DMF, confined in the sample DMF@InOF-1, was experimentally measured by differential scanning calorimetry (DSC) from room temperature to 873 K (with a ramp of 5 K·min^{-1}). The ΔH value was equal to 56.6 kJ·mol^{-1} (see Figure S7 in the Supporting Information). This value is considerably higher than 45.04 kJ·mol^{-1}, which corresponds to the ΔH value for EtOH.[23] The molar enthalpy of vaporization for DMF is 56.7 kJ·mol^{-1}, and the proximity of both enthalpies for DMF (vaporization and adsorption) suggests only one domain of adsorption for DMF, as previously observed for EtOH.[23]

From a practical point of view, the use of DMF@InOF-1 for potential CO_2 capture applications has been shown to be promising because of the high working capacity (approximately 8 wt % CO_2) and very low-cost regeneration conditions (without purge flow and at 303 K). With the intention of investigating more characteristics of DMF@InOF-1 for possible postcombustion CO_2 applications, a series of "key" experiments were performed. First, after the CO_2 adsorption/desorption cycling experiments for DMF@InOF-1 (see Figure 5) were carried out, TGA was performed (see Figure S8 in the Supporting Information) with the motivation of further investigating the residual amount of DMF in the MOF material. TGA showed a DMF residual amount of 4.2 wt %, in good agreement with the residual amount previously observed by Hi-Res TGA experiments (vide supra).

Later, we decided to investigate the stability of DMF@InOF-1 towards H_2O by running a H_2O adsorption isotherm on a freshly synthesized DMF@InOF-1 sample at 303 K (Figure 6).

DOI: 10.1021/acs.inorgchem.7b00519
Inorg. Chem. 2017, 56, 5863–5872

Table 2. Adsorption Properties of PCP Materials Studied Here

sample	BET surface area ($m^2 \cdot g^{-1}$)	pore volume ($cm^3 \cdot g^{-1}$)	CO_2 uptake (303 K, wt %)	ΔH ($kJ \cdot mol^{-1}$)
InOF-1	1066	0.37	5.24	45.6
DMF@InOF-1	628	0.32	8.06	32.4
EtOH@InOF-1	514	0.28	14.14	48.7

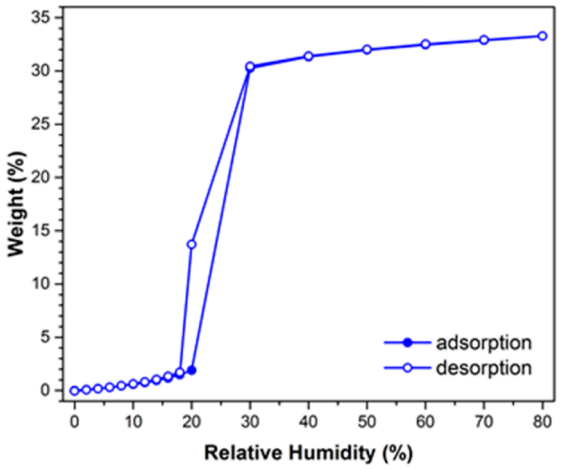

Figure 6. H_2O adsorption isotherm of DMF@InOF-1 with a maximum uptake of 33.3 w%, obtained at 303 K.

The adsorbed amount of H_2O slowly augmented with increasing pressure up to $\%P/P_0$ = 20. Then, a rapid H_2O uptake was observed in the pressure range from $\%P/P_0$ = 20 to 30. Finally, from $\%P/P_0$ = 30 to 80, there was a steady H_2O weight increase, and the maximum H_2O uptake at $\%P/P_0$ = 80 was approximately 33.3 wt %.

The overall H_2O isotherm showed a sigmoidal shape, and a slight hysteresis loop (at $\%P/P_0$ = 20−30) was observed (Figure 6, open circles). Interestingly, this H_2O adsorption isotherm is relatively similar to the one previously reported for an isostructural material entitled NOTT-400.[22d] The maximum H_2O uptake for NOTT-400 was ∼44.9 wt %, which in comparison to DMF@InOF-1 is relatively higher. This result is consistent because the DMF@InOF-1 material hosts DMF (4.2 wt %), and therefore these DMF guest molecules reduce the capacity to adsorb H_2O.

Additionally, after the H_2O adsorption experiment was finished, we decided to evaluate the maximum CO_2 capture on this sample (DMF@InOF-1) by running a kinetic CO_2 uptake experiment (see Figure S9 in the Supporting Information). The total CO_2 capture was equal to 7.4 wt %, which indicated that the total CO_2 uptake for the DMF@InOF-1 sample was slightly reduced (from approximately 8.1 to 7.4 wt %) after being exposed to high amounts of H_2O (80% relative humidity). Therefore, high amounts of H_2O can replace some of the DMF molecules in the DMF@InOF-1 material and, thus, reduce the CO_2 adsorption capacity. However, when the DMF@InOF-1 sample was left for 7 days under ambient conditions (20 °C and 50% relative humidity), the total CO_2 capture (determined by a kinetic CO_2 uptake experiment) was equal to ∼8.1 wt %.

Perhaps the most important parameter for CO_2 post-combustion applications for PCPs is the CO_2 uptake at 0.15 bar and 40 °C and the N_2 uptake at 0.75 bar and the same temperature (40 °C). Then, CO_2 and N_2 adsorption experiments were performed. The CO_2 uptake of DMF@InOF-1 at 0.15 bar and 40 °C was equal to 0.22 $mmol \cdot g^{-1}$, whereas for the fully activated sample (InOF-1), this value was 0.19 $mmol \cdot g^{-1}$. Later, with these experimental measurements, we were able to calculate the adsorption selectivity for CO_2 (α[39]) for both materials. Thus, the uptake values of N_2 at 40 °C and 0.75 bar for the DMF@InOF-1 and InOF-1 samples were 1.4 and 1.8 $mmol \cdot g^{-1}$, respectively. The CO_2 selectivities for these materials were estimated to be α = 0.79 and 0.53 for DMF@InOF-1 and InOF-1, respectively. Certainly, these selectivities are very low in comparison to those of other representative PCPs.[39]

To investigate the CO_2 adsorption properties of DMF@InOF-1, we performed static and isothermal CO_2 adsorption experiments, from 0 to 1 bar at 196 K, on the InOF-1 samples. It was decided to carry out these static CO_2 adsorption experiments at 196 K because the adsorption of CO_2 at 30 °C (303 K) is complex because of the fact that this is just 1 °C below the critical temperature of CO_2.[40] This complexity arises from the uncertainly of the density of the adsorbed phase (CO_2), and the CO_2 saturation pressure is extremely high so that the range of P/P_0 is limited to 0.02 at subatmospheric pressures.[41] Adsorption in fine micropores takes place by a pore-filling mechanism rather than surface coverage.[41,42] For example, N_2 at 77 K can fill these micropores in a liquidlike fashion at very low relative pressures (below 0.01). Conversely, CO_2 adsorbed at around ambient temperatures (298 or 303 K) can only form a monolayer on the walls of the micropores.[42] Thus, in order to achieve pore filling within the micropores of PCPs and, thus, a better description of the CO_2 adsorption properties of these materials, CO_2 gas adsorption experiments at 196 K are preferred.[43]

A CO_2 sorption experiment at 196 K was performed on a fully activated sample of InOF-1 (see Activation Methods in the Supporting Information), exhibiting a total CO_2 uptake of 5.5 $mmol \cdot g^{-1}$ (24.2 wt %; see Figure 7, InOF-1). Later, a newly as-synthesized InOF-1 was placed in a high-pressure cell (Belsorp HP) and activated (453 K and 10^{-3} bar for 1 h) "in situ" to prepare DMF@InOF-1. The CO_2 uptake was measured from 0

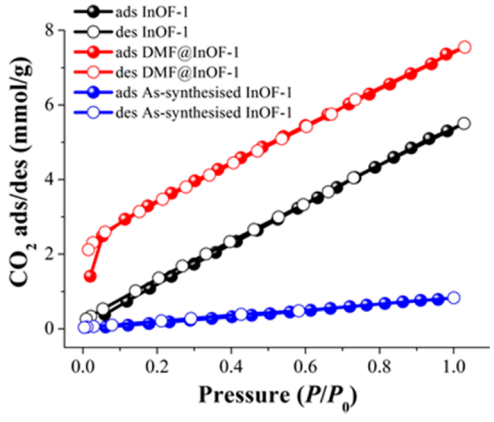

Figure 7. Static CO_2 adsorption/desorption performed from 0 to 1 bar at 196 K on InOF-1 (black circles), DMF@InOF-1 (red circles), and as-synthesized InOF-1 (blue circles): solid circles, adsorption; open circles, desorption.

DOI: 10.1021/acs.inorgchem.7b00519
Inorg. Chem. 2017, 56, 5863−5872

to 1 bar at 196 K, and the resultant CO_2 capture was 7.5 mmol·g^{-1} (33.2 wt %; Figure 7, DMF@InOF-1). Exceptionally, at 1 bar and 196 K, the CO_2 capture was approximately 1.4-fold increased (from 5.5 to 7.5 mmol·g^{-1}) even if part of the pore volume is filled by the residual DMF. The assessment of the BET surface area of DMF@InOF-1 was equal to 628 m^2·g^{-1} with a pore volume of 0.32 cm^3·g^{-1} (lower values than those for the fully activated InOF-1 vide supra, and see Table 2). When these values are compared to those of different PCP materials, DMF@InOF-1 consistently showed, at 196 K, a CO_2 uptake of 7.5 mmol·g^{-1}, which is (in comparison) approximately half of the value for a microporous PCP material entitled PCM-15[44] (14.1 mmol·g^{-1}). However, PCM-15 exhibited a BET surface area of 1187 m^2·g^{-1}, almost double the BET surface area of DMF@InOF-1. An additional example shows that these values for DMF@InOF-1 are also consistent with the results reported for PCM-16,[45] which showed a BET surface area of 1511 m^2·g^{-1} and a CO_2 uptake of 19.8 mmol·g^{-1}. These two values (the BET surface area and CO_2 uptake at 196 K) for PCM-16 are almost 3 times the observed values for DMF@InOF-1.

Finally, an as-synthesized InOF-1 sample was loaded into a high-pressure cell (Belsorp HP). After mild evacuation at room temperature to remove any absorbed moisture, a static CO_2 adsorption isotherm was started at 196 K and 1 bar (Figure 7, as-synthesized InOF-1). The total uptake at 1 bar was approximately 1.0 mmol·g^{-1} (4.4 wt %). This low CO_2 uptake, at the cryogenic temperature of 196 K, signifies adsorption onto the surface of the material. In order to evaluate possible sample degradation after dynamic and static CO_2 capture experiments, PXRD analysis of each sample was carried out, confirming retention of the crystallinity in all samples (see Figure S10 in the Supporting Information).

CONCLUSIONS

When samples of as-synthesized InOF-1 were thermally activated, vide supra, a small residual amount of DMF molecules (confined) was preserved within the pores of InOF-1 (4.2 wt %), affording DMF@InOF-1. Dynamic and isothermal CO_2 experiments on DMF@InOF-1 showed a CO_2 capture of 8.03 wt %, which is approximately 1.5-fold higher than that of a fully activated InOF-1 (5.24%). DMF@InOF-1 can reversibly adsorb/desorb 8.09% CO_2 with no loss of CO_2 capacity after 10 cycles, and the desorption is accomplished by turning the CO_2 flow off without the need for changing the temperature or using inert gas. These properties are the result of the presence of residual DMF molecules in the InOF-1 framework and their interactions via a very strong hydrogen bond with the $In_2(\mu$-OH) groups that prevents DMF leaching and thus conserves the CO_2 sequestration activity even after the 10 cycles. The stability of this hydrogen bond is given by a perfect fit of the DMF molecule in the "dent" around the OH group that allows a nearly perfect orientation of the DMF molecule toward the OH group. Furthermore, static and isothermal CO_2 experiments (from 0 to 1 bar of CO_2 and 196 K) also demonstrated a 1.4-fold CO_2 sequestration increase (from 5.5 mmol·g^{-1}, fully activated InOF-1, to 7.5 mmol·g^{-1}, DMF@InOF-1). The BET surface area for DMF@InOF-1 was estimated to be 628 m^2·g^{-1}, and, interestingly, its CO_2 uptake at 196 K (7.5 mmol·g^{-1}) is very much consistent with PCP materials that exhibited larger BET surface areas (and therefore higher CO_2 uptakes at 196 K), e.g., PCM-15[44] and PCM-16.[45]

Finally, these findings explain the key role of the host−guest interaction in the CO_2 capture and allow the design of more efficient systems working under very mild and reversible conditions. Such work is currently underway.

ASSOCIATED CONTENT

Supporting Information

The Supporting Information is available free of charge on the ACS Publications website at DOI: 10.1021/acs.inorgchem.7b00519.

Experimental details, TGA, Hi-Res TGA, and PXRD data, adsorption microcalorimetry for CO_2 data, DSC for DMF, and postcombustion CO_2 application experiments (PDF)

X-ray crystallographic data in CIF format (CIF)

AUTHOR INFORMATION

Corresponding Authors

*E-mail: egz@xanum.uam.mx (E.G.-Z.).
*E-mail: vjancik@unam.mx (V.J.).
*E-mail: argel@unam.mx (I.A.I.). Fax: +52(55) 5622-4595.

ORCID

Elí Sánchez-González: 0000-0002-5440-329X
Vojtech Jancik: 0000-0002-1007-1764
Ilich A. Ibarra: 0000-0002-8573-8033

Author Contributions

The manuscript was written through contributions of all authors. All authors have given approval to the final version of the manuscript.

Notes

The authors declare no competing financial interest.

ACKNOWLEDGMENTS

The authors thank Dr. A. Tejeda-Cruz (PXRD; IIM-UNAM), CONACyT Mexico (Grant 212318), and PAPIIT UNAM Mexico (Grant IN101517) for financial support. E.G.-Z. thanks CONACyT Mexico (Grant 236879) for financial support. Thanks go to U. Winnberg (ITAM) for scientific discussions. V.J. acknowledges the financial support of CONACyT (Grant 179348). E.S.-G. thanks CONACyT Mexico (Grant 289042).

DEDICATION

This paper is dedicated to Professor Silvia Bulbulian on the occasion of her 87th birthday.

REFERENCES

(1) (a) Chu, S. Carbon Capture and Sequestration. *Science* **2009**, *325*, 1599. (b) Haszeldine, R. S. Carbon Capture and Storage: How Green Can Black Be? *Science* **2009**, *325*, 1647−1652.

(2) Olivier, J. G. J.; Janssens-Maenhout, G.; Muntean, M.; Peters, J. A. H. W. *Trends in Global CO_2 Emissions: 2015 Report*; PBL Netherlands Environmental Assessment Agency: The Hague, The Netherlands, 2015; pp 4−5.

(3) Ertl, G.; Knoezinger, H. *Handbook of Heterogeneous Catalysis*; Wiley-VCH: Weinheim, Germany, 1997; Vol. 5, p 2800.

(4) (a) Kang, X.; Chuang, S. S. C. Transient In Situ IR Study of Selective Catalytic Reduction of NO on Cu-ZSM-5. *Interfacial Applications in Environmental Engineering*; Surfactant Science Series 108; Marcel Dekker: New York, 2003; pp 25−38;. (b) Chi, Y.; Chuang, S. S. C. Infrared Study of NO Adsorption and Reduction with C_3H_6 in the Presence of O_2 over CuO/Al_2O_3. *J. Catal.* **2000**, *190*, 75−91.

(5) (a) D'Alessandro, D. M.; Smit, B.; Long, J. R. Carbon Dioxide Capture: Prospects for New Materials. *Angew. Chem., Int. Ed.* **2010**, *49*, 6058−6082. (b) Sumida, K.; Rogow, D. L.; Mason, J. A.; McDonald,

DOI: 10.1021/acs.inorgchem.7b00519
Inorg. Chem. 2017, 56, 5863−5872

T. M.; Bloch, E. D.; Herm, Z. R.; Bae, T.-H.; Long, J. R. Carbon Dioxide Capture in Metal Organic Frameworks. *Chem. Rev.* **2012**, *112*, 724−781.
(6) (a) Rochelle, G. T. Amine Scrubbing for CO_2 Capture. *Science* **2009**, *325*, 1652−1654. (b) Karadas, F.; Atilhan, M.; Aparicio, S. Review on the Use of Ionic Liquids (ILs) as Alternative Fluids for CO $_2$ Capture and Natural Gas Sweetening. *Energy Fuels* **2010**, *24*, 5817−5828.
(7) Khatri, R. A.; Chuang, S. S. C.; Soong, Y.; Gray, M. Carbon Dioxide Capture by Diamine-Grafted SBA-15: A Combined Fourier Transform Infrared and Mass Spectrometry Study. *Ind. Eng. Chem. Res.* **2005**, *44*, 3702−3708.
(8) Poliakoff, M.; Leitner, W.; Streng, E. S. The Twelve Principles of CO_2 CHEMISTRY. *Faraday Discuss.* **2015**, *183*, 9−17.
(9) (a) Yang, S.; Martin, G. S. B.; Titman, J. J.; Blake, A. J.; Allan, D. R.; Champness, N. R.; Schröder, M. Pore with Gate: Enhancement of the Isosteric Heat of Adsorption of Dihydrogen via Postsynthetic Cation Exchange in Metal−Organic Frameworks. *Inorg. Chem.* **2011**, *50*, 9374−9384. (b) Yang, S.; Lin, X.; Blake, A. J.; Walker, G. S.; Hubberstey, P.; Champness, N. R.; Schröder, M. Cation-Induced Kinetic Trapping and Enhanced Hydrogen Adsorption in a Modulated Anionic Metal−organic Framework. *Nat. Chem.* **2009**, *1*, 487−493. (c) Nuñez, A. J.; Shear, L. N.; Dahal, N.; Ibarra, I. A.; Yoon, J.; Hwang, Y. K.; Chang, J.-S.; Humphrey, S. M. A Coordination Polymer of $(Ph_3P)AuCl$ Prepared by Post-Synthetic Modification and Its Application in 1-Hexene/n-Hexane Separation. *Chem. Commun.* **2011**, *47*, 11855−11857. (d) Lin, X.; Blake, A. J.; Wilson, C.; Sun, X. Z.; Champness, N. R.; George, M. W.; Hubberstey, P.; Mokaya, R.; Schröder, M. A Porous Framework Polymer Based on a Zinc(II) 4,4′-Bipyridine-2,6,2′,6′-Tetracarboxylate: Synthesis, Structure, and "Zeolite-Like" Behaviors. *J. Am. Chem. Soc.* **2006**, *128*, 10745−10753. (e) Nugent, P.; Belmabkhout, Y.; Burd, S. D.; Cairns, A. J.; Luebke, R.; Forrest, K.; Pham, T.; Ma, S.; Space, B.; Wojtas, L.; Eddaoudi, M.; Zaworotko, M. J. Porous Materials with Optimal Adsorption Thermodynamics and Kinetics for CO_2 Separation. *Nature* **2013**, *495*, 80−84. (f) Shekhah, O.; Belmabkhout, Y.; Chen, Z.; Guillerm, V.; Cairns, A.; Adil, K.; Eddaoudi, M. Made-to-Order Metal-Organic Frameworks for Trace Carbon Dioxide Removal and Air Capture. *Nat. Commun.* **2014**, *5*, 4228. (g) Bloch, W. M.; Burgun, A.; Coghlan, C. J.; Lee, R.; Coote, M. L.; Doonan, C. J.; Sumby, C. J. Capturing Snapshots of Post-Synthetic Metallation Chemistry in Metal−organic Frameworks. *Nat. Chem.* **2014**, *6*, 906−912. (h) Okada, K.; Ricco, R.; Tokudome, Y.; Styles, M. J.; Hill, A. J.; Takahashi, M.; Falcaro, P. Copper Conversion into $Cu(OH)_2$ Nanotubes for Positioning $Cu_3(BTC)_2$ MOF Crystals: Controlling the Growth on Flat Plates, 3D Architectures, and as Patterns. *Adv. Funct. Mater.* **2014**, *24*, 1969−1977. (i) Li, H.; Hill, M. R.; Huang, R.; Doblin, C.; Lim, S.; Hill, A. J.; Babarao, R.; Falcaro, P. Facile Stabilization of Cyclodextrin Metal−organic Frameworks under Aqueous Conditions via the Incorporation of C_{60} in Their Matrices. *Chem. Commun.* **2016**, *52*, 5973−5976. (j) Sumida, K.; Moitra, N.; Reboul, J.; Fukumoto, S.; Nakanishi, K.; Kanamori, K.; Furukawa, S.; Kitagawa, S. Mesoscopic Superstructures of Flexible Porous Coordination Polymers Synthesized via Coordination Replication. *Chem. Sci.* **2015**, *6*, 5938−5946. (k) Hirai, K.; Furukawa, S.; Kondo, M.; Uehara, H.; Sakata, O.; Kitagawa, S. Sequential Functionalization of Porous Coordination Polymer Crystals. *Angew. Chem., Int. Ed.* **2011**, *50*, 8057−8061. (l) Nguyen, N. T. T.; Lo, T. N. H.; Kim, J.; Nguyen, H. T. D.; Le, T. B.; Cordova, K. E.; Furukawa, H. Mixed-Metal Zeolitic Imidazolate Frameworks and Their Selective Capture of Wet Carbon Dioxide over Methane. *Inorg. Chem.* **2016**, *55*, 6201−6207. (m) Seth, S.; Savitha, G.; Moorthy, J. N. Carbon Dioxide Capture by a Metal−Organic Framework with Nitrogen-Rich Channels Based on Rationally Designed Triazole-Functionalized Tetraacid Organic Linker. *Inorg. Chem.* **2015**, *54*, 6829−6835.
(10) (a) Tozawa, T.; Jones, J. T. A.; Swamy, S. I.; Jiang, S.; Adams, D. J.; Shakespeare, S.; Clowes, R.; Bradshaw, D.; Hasell, T.; Chong, S. Y.; Tang, C.; Thompson, S.; Parker, J.; Trewin, A.; Bacsa, J.; Slawin, A. M. Z.; Steiner, A.; Cooper, A. I. Porous Organic Cages. *Nat. Mater.* **2009**, *8*, 973−978. (b) Dawson, R.; Adams, D. J.; Cooper, A. I. Chemical Tuning of CO_2 Sorption in Robust Nanoporous Organic Polymers. *Chem. Sci.* **2011**, *2*, 1173−1177. (c) Bloch, W. M.; Babarao, R.; Hill, M. R.; Doonan, C. J.; Sumby, C. J. Post-Synthetic Structural Processing in a Metal−Organic Framework Material as a Mechanism for Exceptional CO_2 /N $_2$ Selectivity. *J. Am. Chem. Soc.* **2013**, *135*, 10441−10448. (d) Mason, J. A.; Sumida, K.; Herm, Z. R.; Krishna, R.; Long, J. R. Evaluating Metal−organic Frameworks for Post-Combustion Carbon Dioxide Capture via Temperature Swing Adsorption. *Energy Environ. Sci.* **2011**, *4*, 3030−3040.
(11) (a) Demessence, A.; D'Alessandro, D. M.; Foo, M. L.; Long, J. R. Strong CO_2 Binding in a Water-Stable, Triazolate-Bridged Metal−Organic Framework Functionalized with Ethylenediamine. *J. Am. Chem. Soc.* **2009**, *131*, 8784−8786. (b) Zhang, J.-P.; Chen, X.-M. Optimized Acetylene/Carbon Dioxide Sorption in a Dynamic Porous Crystal. *J. Am. Chem. Soc.* **2009**, *131*, 5516−5521. (c) Seth, S.; Savitha, G.; Moorthy, J. N. Carbon Dioxide Capture by a Metal−Organic Framework with Nitrogen-Rich Channels Based on Rationally Designed Triazole-Functionalized Tetraacid Organic Linker. *Inorg. Chem.* **2015**, *54*, 6829−6835.
(12) Vaidhyanathan, R.; Iremonger, S. S.; Shimizu, G. K. H.; Boyd, P. G.; Alavi, S.; Woo, T. K. Direct Observation and Quantification of CO_2 Binding Within an Amine-Functionalized Nanoporous Solid. *Science* **2010**, *330*, 650−653.
(13) Pachfule, P.; Banerjee, R. Porous Nitrogen Rich Cadmium-Tetrazolate Based Metal Organic Framework (MOF) for H_2 and CO_2 Uptake. *Cryst. Growth Des.* **2011**, *11*, 5176−5181.
(14) (a) Suh, M. P.; Park, H. J.; Prasad, T. K.; Lim, D.-W. Hydrogen Storage in Metal−Organic Frameworks. *Chem. Rev.* **2012**, *112*, 782−835. (b) Dincă, M.; Long, J. R. Hydrogen Storage in Microporous Metal-Organic Frameworks with Exposed Metal Sites. *Angew. Chem., Int. Ed.* **2008**, *47*, 6766−6779. (c) Ibarra, I. A.; Lin, X.; Yang, S.; Blake, A. J.; Walker, G. S.; Barnett, S. A.; Allan, D. R.; Champness, N. R.; Hubberstey, P.; Schröder, M. Structures and H_2 Adsorption Properties of Porous Scandium Metal-Organic Frameworks. *Chem. - Eur. J.* **2010**, *16*, 13671−13679. (d) Park, J.; Kim, H.; Han, S. S.; Jung, Y. Tuning Metal−Organic Frameworks with Open-Metal Sites and Its Origin for Enhancing CO_2 Affinity by Metal Substitution. *J. Phys. Chem. Lett.* **2012**, *3*, 826−829. (e) Kong, X.; Scott, E.; Ding, W.; Mason, J. A.; Long, J. R.; Reimer, J. A. CO_2 Dynamics in a Metal−Organic Framework with Open Metal Sites. *J. Am. Chem. Soc.* **2012**, *134*, 14341−14344. (f) Ibarra, I. A.; Tan, K. E.; Lynch, V. M.; Humphrey, S. M. CO_2 Adsorption Properties of a Ca(II)-Based Organophosphonium Coordination Material. *Dalt. Trans.* **2012**, *41*, 3920−3923. (g) López-Olvera, A.; Sánchez-González, E.; Campos-Reales-Pineda, A.; Aguilar-Granda, A.; Ibarra, I. A.; Rodríguez-Molina, B. CO_2 Capture in a Carbazole-Based Supramolecular Polyhedron Structure: The Significance of Cu(II) Open Metal Sites. *Inorg. Chem. Front.* **2017**, *4*, 56−64.
(15) (a) Ho, N. L.; Perez-Pellitero, J.; Porcheron, F.; Pellenq, R. J.-M. Enhanced CO_2 Solubility in Hybrid Adsorbents: Optimization of Solid Support and Solvent Properties for CO_2 Capture. *J. Phys. Chem. C* **2012**, *116*, 3600−3607. (b) Ho, L. N.; Perez Pellitero, J.; Porcheron, F.; Pellenq, R. J.-M. Enhanced CO_2 Solubility in Hybrid MCM-41: Molecular Simulations and Experiments. *Langmuir* **2011**, *27*, 8187−8197. (c) Ho, N. L.; Porcheron, F.; Pellenq, R. J.-M. Experimental and Molecular Simulation Investigation of Enhanced CO_2 Solubility in Hybrid Adsorbents. *Langmuir* **2010**, *26*, 13287−13296.
(16) (a) Volino, F.; Gérard, H.; Miachon, S. Non-Extensive Visco-Elastic Theory II. First Experimental Tests of the Simple Theory with Rotational Modes. *Ann. Phys.* **1997**, *22*, 43−82. (b) Morishige, K.; Shikimi, M. Adsorption Hysteresis and Pore Critical Temperature in a Single Cylindrical Pore. *J. Chem. Phys.* **1998**, *108*, 7821−7824. (c) Kimball, M. O.; Gasparini, F. M. Universality and Finite-Size Scaling of the Specific Heat of ^{3}He−^{4}He Mixtures. *Phys. Rev. Lett.* **2005**, *95*, 165701. (d) Zammit, U.; Marinelli, M.; Mercuri, F.; Paoloni, S. Effect of Confinement and Strain on the Specific Heat and Latent Heat over the Nematic−Isotropic Phase Transition of 8CB Liquid Crystal. *J. Phys. Chem. B* **2009**, *113*, 14315−14322.

DOI: 10.1021/acs.inorgchem.7b00519
Inorg. Chem. 2017, 56, 5863−5872

(17) (a) Luzar, A.; Bratko, D. Gas Solubility in Hydrophobic Confinement. *J. Phys. Chem. B* **2005**, *109*, 22545−22552. (b) Bratko, D.; Luzar, A. Attractive Surface Force in the Presence of Dissolved Gas: A Molecular Approach. *Langmuir* **2008**, *24*, 1247−1253.
(18) Soubeyrand-Lenoir, E.; Vagner, C.; Yoon, J. W.; Bazin, P.; Ragon, F.; Hwang, Y. K.; Serre, C.; Chang, J. S.; Llewellyn, P. L. How Water Fosters a Remarkable 5-Fold Increase in Low-Pressure CO_2 Uptake within Mesoporous MIL-100(Fe). *J. Am. Chem. Soc.* **2012**, *134*, 10174−10181.
(19) (a) Jasuja, H.; Huang, Y.; Walton, K. S. Adjusting the Stability of Metal−Organic Frameworks under Humid Conditions by Ligand Functionalization. *Langmuir* **2012**, *28*, 16874−16880. (b) Jasuja, H.; Zang, J.; Sholl, D. S.; Walton, K. S. Rational Tuning of Water Vapor and CO_2 Adsorption in Highly Stable Zr-Based MOFs. *J. Phys. Chem. C* **2012**, *116* (44), 23526−23532. (c) DeCoste, J. B.; Peterson, G. W.; Jasuja, H.; Glover, T. G.; Huang, Y.; Walton, K. S. Stability and Degradation Mechanisms of Metal−organic Frameworks Containing the $Zr_6O_4(OH)_4$ Secondary Building Unit. *J. Mater. Chem. A* **2013**, *1*, 5642. (d) Burtch, N. C.; Jasuja, H.; Walton, K. S. Water Stability and Adsorption in Metal−Organic Frameworks. *Chem. Rev.* **2014**, *114*, 10575−10612.
(20) Cmarik, G. E.; Kim, M.; Cohen, S. M.; Walton, K. S. Tuning the Adsorption Properties of UiO-66 via Ligand Functionalization. *Langmuir* **2012**, *28*, 15606−15613.
(21) Furukawa, H.; Gándara, F.; Zhang, Y.-B.; Jiang, J.; Queen, W. L.; Hudson, M. R.; Yaghi, O. M. Water Adsorption in Porous Metal-Organic Frameworks and Related Materials. *J. Am. Chem. Soc.* **2014**, *136*, 4369−4381.
(22) (a) Gonzalez, M. R.; González-Estefan, J. H.; Lara-García, H. A.; Sánchez-Camacho, P.; Basaldella, E. I.; Pfeiffer, H.; Ibarra, I. A. Separation of CO_2 from CH_4 and CO_2 Capture in the Presence of Water Vapour in NOTT-400. *New J. Chem.* **2015**, *39*, 2400−2403. (b) Lara-García, H. A.; Gonzalez, M. R.; González-Estefan, J. H.; Sánchez-Camacho, P.; Lima, E.; Ibarra, I. A. Removal of CO_2 from CH_4 and CO_2 Capture in the Presence of H_2O Vapour in NOTT-401. *Inorg. Chem. Front.* **2015**, *2*, 442−447. (c) Peralta, R. A.; Alcántar-Vázquez, B.; Sánchez-Serratos, M.; González-Zamora, E.; Ibarra, I. A. Carbon Dioxide Capture in the Presence of Water Vapour in InOF-1. *Inorg. Chem. Front.* **2015**, *2*, 898−903. (d) Álvarez, J. R.; Peralta, R. A.; Balmaseda, J.; González-Zamora, E.; Ibarra, I. A. Water Adsorption Properties of a Sc(III) Porous Coordination Polymer for CO_2 Capture Applications. *Inorg. Chem. Front.* **2015**, *2*, 1080−1084. (e) Sánchez-Serratos, M.; Bayliss, P. a.; Peralta, R. a.; González-Zamora, E.; Lima, E.; Ibarra, I. a. CO_2 Capture in the Presence of Water Vapour in MIL-53(Al). *New J. Chem.* **2016**, *40*, 68. (f) Zárate, A.; Peralta, R. A.; Bayliss, P. A.; Howie, R.; Sánchez-Serratos, M.; Carmona-Monroy, P.; Solis-Ibarra, D.; González-Zamora, E.; Ibarra, I. A. CO_2 Capture under Humid Conditions in NH_2-MIL-53(Al): The Influence of the Amine Functional Group. *RSC Adv.* **2016**, *6*, 9978−9983. (g) Sánchez-González, E.; Álvarez, J. R.; Peralta, R. A.; Campos-Reales-Pineda, A.; Tejeda-Cruz, A.; Lima, E.; Balmaseda, J.; González-Zamora, E.; Ibarra, I. A. Water Adsorption Properties of NOTT-401 and CO_2 Capture under Humid Conditions. *ACS Omega* **2016**, *1*, 305−310. (h) González-Zamora, E.; Ibarra, I. A. CO_2 capture under humid conditions in metal−organic frameworks. *Mater. Chem. Front.* **2017**, *XX*, XXX DOI: 10.1039/C6QM00301J.
(23) Peralta, R. A.; Campos-Reales-Pineda, A.; Pfeiffer, H.; Álvarez, J. R.; Zárate, J. A.; Balmaseda, J.; González-Zamora, E.; Martínez, A.; Martínez-Otero, D.; Jancik, V.; Ibarra, I. A. CO_2 Capture Enhancement in InOF-1 via the Bottleneck Effect of Confined Ethanol. *Chem. Commun.* **2016**, *52*, 10273−10276.
(24) Qian, J.; Jiang, F.; Yuan, D.; Wu, M.; Zhang, S.; Zhang, L.; Hong, M. Highly Selective Carbon Dioxide Adsorption in a Water-Stable Indium−organic Framework Material. *Chem. Commun.* **2012**, *48*, 9696.
(25) Lin, X.; Telepeni, I.; Blake, A. J.; Dailly, A.; Brown, C. M.; Simmons, J. M.; Zoppi, M.; Walker, G. S.; Thomas, K. M.; Mays, T. J.; Hubberstey, P.; Champness, N. R.; Schröder, M. High Capacity Hydrogen Adsorption in Cu(II) Tetracarboxylate Framework Materials: The Role of Pore Size, Ligand Functionalization, and Exposed Metal Sites. *J. Am. Chem. Soc.* **2009**, *131*, 2159−2171.
(26) *APEX, SAINT and SADABS*; Bruker AXS Inc.: Madison, WI, 2015.
(27) Sheldrick, G. M. *SHELXT* − Integrated space-group and crystal-structure determination. *Acta Crystallogr., Sect. A: Found. Adv.* **2015**, *71*, 3−8.
(28) Sheldrick, G. M. Crystal structure refinement with *SHELXL*. *Acta Crystallogr., Sect. C: Struct. Chem.* **2015**, *71*, 3−8.
(29) Hübschle, C. B.; Sheldrick, G. M.; Dittrich, B. *ShelXle*: A Qt Graphical User Interface for *SHELXL*. *J. Appl. Crystallogr.* **2011**, *44*, 1281−1284.
(30) *GIMP: The GNU Image Manipulation Program*, version 2.8; The GIMP Development Team, 2012; http://www.gimp.org (Jan 9, 2017).
(31) Macrae, C. F.; Bruno, I. J.; Chisholm, J. A.; Edgington, P. R.; McCabe, P.; Pidcock, E.; Rodriguez-Monge, L.; Taylor, R.; van de Streek, J.; Wood, P. A. *Mercury CSD 2.0* − New Features for the Visualization and Investigation of Crystal Structures. *J. Appl. Crystallogr.* **2008**, *41*, 466−470.
(32) Medders, G. R.; Paesani, F. Water Dynamics in Metal−Organic Frameworks: Effects of Heterogeneous Confinement Predicted by Computational Spectroscopy. *J. Phys. Chem. Lett.* **2014**, *5*, 2897−2902.
(33) Haigis, V.; Coudert, F.-X.; Vuilleumier, R.; Boutin, A. Investigation of Structure and Dynamics of the Hydrated Metal-Organic Framework MIL-53(Cr) Using First-Principles Molecular Dynamics. *Phys. Chem. Chem. Phys.* **2013**, *15*, 19049−19056.
(34) Salles, F.; Bourrelly, S.; Jobic, H.; Devic, T.; Guillerm, V.; Llewellyn, P.; Serre, C.; Ferey, G.; Maurin, G. Molecular Insight into the Adsorption and Diffusion of Water in the Versatile Hydrophilic/Hydrophobic Flexible MIL-53(Cr) MOF. *J. Phys. Chem. C* **2011**, *115*, 10764−10776.
(35) Metz, B.; Davidson, O.; Coninck, H.; de Loos, M.; Meyer, L. *IPCC, 2005: IPCC Special Report on Carbon Dioxide Capture and Storage*; Cambridge University Press: Cambridge, U.K., 2005.
(36) McDonald, T. M.; D'Alessandro, D. M.; Krishna, R.; Long, J. R. Enhanced Carbon Dioxide Capture upon Incorporation of *N,N′*-Dimethylethylenediamine in the Metal−organic Framework CuBTTri. *Chem. Sci.* **2011**, *2*, 2022−2028.
(37) Britt, D.; Furukawa, H.; Wang, B.; Glover, T. G.; Yaghi, O. M. Highly Efficient Separation of Carbon Dioxide by a Metal-Organic Framework Replete with Open Metal Sites. *Proc. Natl. Acad. Sci. U. S. A.* **2009**, *106*, 20637−20640.
(38) Couck, S.; Denayer, J. F. M.; Baron, G. V.; Rémy, T.; Gascon, J.; Kapteijn, F. An Amine-Functionalized MIL-53 Metal−Organic Framework with Large Separation Power for CO_2 and CH_4. *J. Am. Chem. Soc.* **2009**, *131*, 6326−6327.
(39) Ibarra, I. A.; Mace, A.; Yang, S.; Sun, J.; Lee, S.; Chang, J.-S.; Laaksonen, A.; Schröder, M.; Zou, X. *Inorg. Chem.* **2016**, *55*, 7219.
(40) *CRC Handbook of Chemistry and Physics*, 85th ed.; Lide, D. R., Ed.; CRC Press: Boca Raton, FL, 2004.
(41) Rouquerol, F.; Rouquerol, J.; Sing, K. S. W.; Llewellyn, P.; Maurin, G. *Adsorption by Powders and Porous Solids; Principles, Methodology and Applications*, 2nd ed.; Academic Press: Oxford, U.K., 2014.
(42) Garrido, J.; Linares-Solano, A.; Martín-Martínez, J. M.; Molina-Sabio, M.; Rodríguez-Reinoso, F.; Torregrosa, R. Use of nitrogen vs. carbon dioxide in the characterization of activated carbons. *Langmuir* **1987**, *3*, 76−81.
(43) (a) Park, H. J.; Suh, M. P. Mixed-Ligand Metal-Organic Frameworks with Large Pores: Gas Sorption Properties and Single-Crystal-to-Single-Crystal Transformation on Guest Exchange. *Chem. - Eur. J.* **2008**, *14*, 8812−8821. (b) Humphrey, S. M.; Chang, J. S.; Jhung, S. H.; Yoon, J. W.; Wood, P. T. Porous cobalt(II)-Organic Frameworks with Corrugated Walls: Structurally Robust Gas-Sorption Materials. *Angew. Chem., Int. Ed.* **2007**, *46*, 272−275. (c) Lee, J.; Waggoner, N. W.; Polanco, L.; You, G. R.; Lynch, V. M.; Kim, S. K.; Humphrey, S. M.; Sessler, J. L. Ship in a Breakable Bottle: Fluoride-Induced Release of an Organic Molecule from a Pr(III)-Linked Molecular Cage. *Chem. Commun.* **2016**, *52*, 8514−8517.

DOI: 10.1021/acs.inorgchem.7b00519
Inorg. Chem. 2017, 56, 5863−5872

(44) (a) Ibarra, I. A.; Hesterberg, T. W.; Chang, J.-S.; Yoon, J. W.; Holliday, B. J.; Humphrey, S. M. Molecular Sensing and Discrimination by a Luminescent Terbium-Phosphine Oxide Coordination Material. *Chem. Commun.* **2013**, *49*, 7156−7158. (b) Ibarra, I. A.; Hesterberg, T. W.; Chang, J.-S.; Yoon, J. W.; Holliday, B. J.; Humphrey, S. M.; Zhang, J.; Williams, J. A. G.; Woods, M.; Huberstey, P.; Champness, N. R.; Thomas, K. M.; Blake, A. J.; Schröder, M. Molecular Sensing and Discrimination by a Luminescent Terbium−phosphine Oxide Coordination Material. *Chem. Commun.* **2013**, *49*, 7156.

(45) Ibarra, I. A.; Yoon, J. W.; Chang, J.-S.; Lee, S. K.; Lynch, V. M.; Humphrey, S. M. Organic Vapor Sorption in a High Surface Area Dysprosium(III)−Phosphine Oxide Coordination Material. *Inorg. Chem.* **2012**, *51*, 12242−12247.

DOI: 10.1021/acs.inorgchem.7b00519
Inorg. Chem. 2017, 56, 5863−5872